Theoretical Determination of the Standard Reduction Potential of Plastocyanin in Vitro

Sambhu N. Datta,* Jawahar Sudhamsu, and Anshu Pandey

Department of Chemistry, Indian Institute of Technology, Bombay, Powai, Mumbai 400076, India

Received: June 11, 2003; In Final Form: March 3, 2004

Quantum chemical QM/MM calculations have been performed on the copper-containing blue protein plastocyanin that is involved in the photosynthetic electron transfer. Crystallographic coordinates of the non-hydrogen atoms in the oxidized and reduced forms of poplar plastocyanin were obtained from the Protein Data Bank. The present work required calculations on the oxidized form that has a molecular structure independent of pH, and the reduced form with different structures at pH values 3.8 and 7. At pH 7, both the oxidized and reduced forms of the protein have distorted tetrahedral geometry for the copper-containing active site, the Cu atom being coordinated to two histidine, one cysteine, and one methionine residues. At pH 3.8, the active site of the reduced species is trigonally coordinated to one histidine, one cysteine, and one methionine residues. To optimize the geometry of the system while retaining the constraints of the protein backbone, the ONIOM methodology was adopted so as to treat the active site by the DFT-B3LYP method using the 6-31G basis set, whereas the geometries of the nearby residues as well as six neighboring water molecules were optimized by the MM/UFF method. Then atomic charges for the atoms of the protein (apart from those in the active site) were determined from DFT calculations separately for each amino acid residue using the STO-3G basis set. The atomic charges of the water molecules were computed by the DFT/6-31G(d) method. Finally, the electronic energies were recalculated by the ONIOM technique where the DFT-optimized active site was again treated at the 6-31G level of theory, whereas the rest of the protein, along with the solvent molecules near the active site, were treated by the Amber force field method using the calculated DFT charge on each atom. This treatment effectively allowed us to retain the steric constraints offered by the protein backbone during the optimization process, as well as the effects arising from the interaction of the protein dipoles and the bare charges on the protein with the atomic charges in the complex, thereby accommodating all electronic interactions such as charge−charge, charge-dipole, dipole−dipole, etc. The thermal energies of various oxidized and reduced forms were computed for a slightly simplified model of the active site (the part optimized in ONIOM) by using the DFT-B3LYP methodology. The effective radius of the globular protein plastocyanin was determined from the crystallographic data. The stability of each species arising from its interaction with medium was determined by explicitly calculating the Born charge−dielectric (water) interaction energy and, for the solvated proton, the Debye−Hückel energy of ion−ionic atmosphere interaction. The dielectric constant of water and plastocyanin were taken as 78.5 and 8.0, respectively. The interaction with the medium and the entropy changes are found to play a critical role in determining the reduction potential. The process of reduction of plastocyanin in an aqueous medium involves a very large reorganization of water molecules, and a large entropy change that cannot be computed readily. Hence, the entropy of reduction of plastocyanin was taken from experimental data that are available for pH 7. The free energy change was calculated for the reduction of plastocyanin in water and proton in water. From these values, the standard reduction potential was determined at pH 7. The calculated potential (376 ± 38 mV) is in excellent agreement with the observed one (379 mV) for the radius of the globular protein 22.37 ± 0.16 Å. A similar calculation leads us to predict the entropy of reduction of plastocyanin at pH 3.8.

1. Introduction

Plastocyanin (PC) is a 97−99 residue redox active protein[1] that stays in the aqueous phase of chloroplast, near the thylakoid membrane. It is the redox partner of cytochrome *f* and P700 in the Z scheme of photosynthesis. It accepts an electron from cytochrome *f* that is embedded in the condensed phase of the thylakoid membrane and then migrates through the stroma to reach Photosystem I, that is, P700. Spectroscopic studies on the soluble type 1 blue copper protein have shown an intense absorption band near 600 nm and a midpoint reduction potential of 0.379 V at 25 °C at pH 7.[2]

Plastocyanin from poplar leaves is a protein with a single polypeptide chain, has a molecular weight around 10 500 Da, and resembles a slightly flattened spheroid. The crystal structure of poplar plastocyanin in its oxidized form and that of the reduced forms at various pH have been reported.[3] Recent structure analyses of the oxidized form of plastocyanin at different pH values showed that the oxidized Cu site was, within the limits of precision, invariant in the range $4.2 \leq \text{pH} \leq 6.0$.[4] The most significant differences among the structures of the reduced protein at different pH values, or between them and the structure of the oxidized protein, are concentrated at the Cu site. In both the oxidized and reduced forms at high pH, the Cu atom is coordinated by the N^{δ} (imidazole) atoms of His37 and

* Corresponding author. E-mail: sndatta@chem.iitb.ac.in.

10.1021/jp0307452 CCC: $27.50
Published on Web 05/18/2004

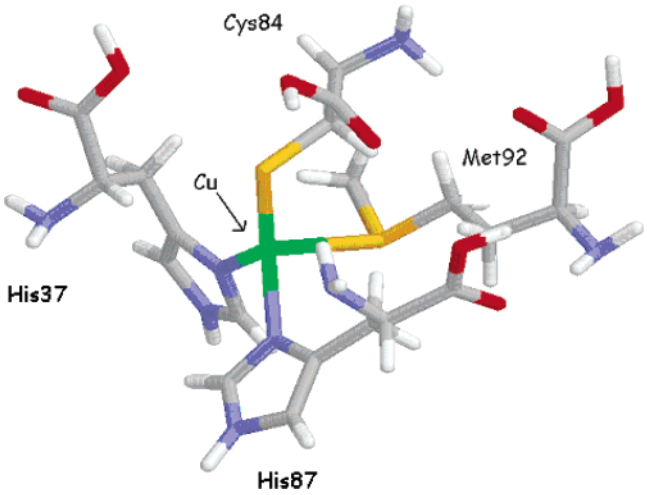

Figure 1. Active site in plastocyanin, with the binding residues modeled as amino acids. The stereoscopic projection is shown here.

His87, the S^{γ} (thiolate) atom of Cys84, and the S^{δ} (thioether) atom of Met92 (Figure 1). The distorted tetrahedral geometry and the unusually long Cu−S (Met92) bond are retained in both these forms. The only effects of the reduction at a high pH are a lengthening of the two Cu−N (His) bonds by about 0.1 Å, and small changes in two bond angles involving the Cu−S (Cys) bond. As the pH is lowered, the Cu atom and the four Cu-binding side chains appear to undergo small but concerted movements in relation to the rest of the molecule. At a low pH (pH 3.8), the reduced form has the Cu atom trigonally coordinated by N^{δ} (His37), S^{γ} (Cys84), and S^{δ} (Met92). The fourth Cu−ligand bond is broken, the Cu atom making only a van der Waals contact with the imidazole ring of His87. The imidazole ring is rotated by 180° about the $C^{\beta}-C^{\gamma}$ bond with respect to its orientation in the high-pH form and is protonated.[5]

It is known that plastocyanin has a pH-dependent reduction potential below pH 5.5.[6] Plastocyanins from different sources show somewhat varying redox potentials. For example, whereas poplar plastocyanin has a redox potential of 441 mV at pH 3.6, plastocyanins from cucumber, spinach, and parsley show slightly different values of 458, 473, and 497 mV, respectively, at the same pH. Similar trends are noticed for other pH values.[6c] Reference 6c shows that at pH 7, plastocyanin from *Populus nigra* variant *italica* has a midpoint potential of 0.379 V. The rate of reaction between the reduced form of plastocyanin and inorganic oxidants depends on the pH value, and the existence of a protonated redox-inactive form of the protein was proposed earlier.[7] It is now contended that in aqueous solution and below pH 5.5, the redox-active high-pH form and the redox-inactive low-pH form must be in a dynamic equilibrium. Also, the fact that the structural changes related to the oxidation state or pH must be highly localized is supported by independent evidence from ^{13}C and ^{1}H nuclear magnetic resonance measurements on the oxidized and reduced forms of plastocyanin in solution.[8] Plastocyanins from different sources have been electrochemically characterized, and their reduction potentials at different pH are known.[6]

One important feature of the protein is that in solution, it is highly charged in the pH range 2−10. In general, the amino group in the side chain of lysine and arginine residues in a protein is protonated at pH ≤ 10 if it is exposed to the solvent. For histidine residues the δ nitrogen atom is protonated at pH ≤ 6. Similarly, the carboxylate groups in the side chains of solvent-exposed glutamic acid and aspartic acid residues are deprotonated at pH ≥ 2.0. Figure 2 shows the active site and

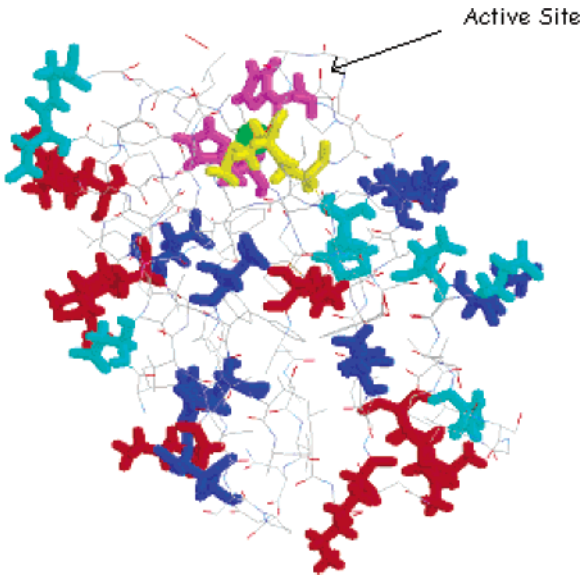

Figure 2. Charged surface residues are shown in stick model along with the active site. The rest of the protein is in the wire model.

the charged residues in the stick model and the rest of the protein in the wire model. Poplar plastocyanin has seven aspartic acids, eight glutamic acids, and six lysine residues but no arginine residue. The two histidine residues are bound to the metal and hence they are not protonated at the physiological pH.

As a part of our ongoing investigations on the redox processes occurring in the Z-scheme,[9−13] we have theoretically determined the reduction potential of plastocyanin by using the quantum mechanics/molecular mechanics (QM/MM) method. The molecular structure selected for our quantum chemical calculation is discussed in section 2. A short discussion on the method of calculation is given in section 3. The computed results are presented in section 4. The energies and the molecular orbitals computed in this work will be used to determine the rates of electron transfer from cytochrome *f* to plastocyanin and finally from plastocyanin to P700. Our conclusions are summarized in section 5, where we also discuss the limitations of the present work in detail.

2. Molecular Geometry

Crystallographic Geometry. The basic aim of this work is to calculate the reduction potential of plastocyanin in vitro. Whereas the crystallographic structure represents the structure of the biomolecule in a condensed phase, it is also known to be very unreliable for proteins in solution, and thus it becomes necessary to optimize the geometry of the protein model used for computations. A significant problem involved is that of retention of the protein backbone during the optimization process for the geometry of the active site and its immediate environs. To effectively retain the geometry constraints, we used an ONIOM methodology to simulate the nearby residues of the protein at a low level of theory, namely, the molecular mechanics/universal force field (MM/UFF) method, while modeling the active site at a high level of theory, namely, density functional treatment (DFT). The starting points of the optimizations were the protein crystallographic coordinates at different pH values. Crystallographic coordinates were obtained from the Protein Data Bank at Brookhaven National Laboratory (PDB Code: 1PLC of the plastocyanin in oxidized form at pH 6.0, 5PCY of plastocyanin in reduced form at pH 7.0, and 6PCY of plastocyanin in reduced form at pH 3.8 from poplar leaves, *P. nigra* variant *italica*).

The copper-containing active site is close to the surface of the molecule and is coordinated to a surface exposed histidinyl (His-87) imidazole moiety. The three other coordinating atoms are a cysteinyl (Cys-84) thiolate, a methioninyl (Met-92) sulfur and another histidinyl (His-37) imidazole, as shown in Figure 1. The geometry is a distorted tetrahedron. This distortion is thought to be responsible for the relatively high midpoint potential of the protein. More recently, the abnormally long copper−thioether axial bond has also been cited as a key factor responsible for the relatively high midpoint potential of the protein.[14] The free energy of reduction must be predominantly determined by the electronic structure of the Cu complex, which is the redox center. The same free energy, nevertheless, is a small quantity and so its magnitude is greatly influenced by the surrounding protein chain. The interaction between the complex and the enveloping proteinous part is mainly electrostatic in nature. Hence the calculation of the electronic structure of the complexes, though exhaustively accounting for the interaction with the medium, is expected to give rise to a reasonably good estimate of the reduction potential.

Model Complexes. The present work required calculations on the oxidized form that has a structure independent of pH, and the reduced form with different structures at pH values 3.8 and 7.

The structure of the oxidized form was reported to be essentially invariant in the pH range $4.2 \leq 6$.[6] In this work we assume that the structure of the oxidized form also holds for the pH range 3.8−7, in which we are computing the reduction potentials.

The contribution of the protein backbone to the evolution of the geometry of the active site was simulated at first by including the nearby residues in the optimization process. Thus, the residues proline 36, aspargine 38, tyrosine 83, serine 85, proline 86, glutamine 88, glycine 91, and valine 93, as well as a number of solvent molecules (six) were included in the model and treated at a low level of theory, namely, the molecular mechanics/universal force field (MM/UFF) method, during the optimization. The active site containing the Cu atom, the histidine imidazole rings, and the cysteine $-S-CH_2$ and methionine CH_3-S-CH_2 groups (modeled in ONIOM as $-S-CH_3$ and $S(CH_3)_2$, respectively) as shown in Figure 3 were studied by the DFT/B3LYP methodology. The neighbors and the active site for the first set of ONIOM calculations are shown in Figure 4 for the oxidized species. The DFT atomic charges on the protein were computed separately for each amino acid residue using the STO-3G basis set, with the individual amino acids being modeled as amino aldehydes, as suggested by the reviewers. The N terminal of the amide linkages were clipped to amines, whereas the carboxylate terminals were treated as aldehydes. Similarly, atomic charges of the water molecules were computed by the DFT/6-31G(d) method. The electronic energies were determined by treating the DFT-optimized region at a 6-31G level of theory, but the rest of the protein, along with the 44 solvent molecules near the active site (which had been previously optimized by Amber force field), were now treated as point charges. This procedure not only keeps up the steric constraints offered by the protein backbone but also accommodates all electronic interactions such as charge−charge, charge−dipole, dipole−dipole, etc. The final model complex for the oxidized form is shown in Figure 5.

3. Method of Calculation

Methodology. For more than two decades, ab initio,[15−21] semiempirical,[22−25] and even empirical[26−32] methods have been used to compute electronic coupling interactions in long-distance electron transfer processes such as those involved in photosynthesis. The calculation of the redox potentials of biomolecules that are generally large species is a notoriously difficult job. In the theoretical studies of large systems, smaller models of the real systems have been traditionally employed. In the case of a system as large as a protein, the underlying problem is to retain the effects of the large protein chain on the active site while simulating the active site at a high level of theory. The ONIOM method offers an attractive technique to effectively study the characteristics of a large biological system, by dividing the system into components or layers, which are studied at differing levels of theory. The ONIOM[33] method expresses the energy of the system as

$$E(\mathrm{ONIOM}n) = \sum_{i=1}^{n} E[\mathrm{Level}(i),\mathrm{Model}(n+1-i)] - \sum_{j=1}^{n} E[\mathrm{Level}(j),\mathrm{Model}(n+2-j)] \quad (1)$$

During geometry optimization of the active site, we have simulated the system by a two-layer ONIOM, in which the active site is studied using density functional theory, whereas the lower layer consisting of adjoining residues is treated by using molecular mechanics. Density functional theory (DFT) has revolutionized studies on transition metal complexes and proteins (especially blue copper proteins), providing much more accurate results at approximately the same cost as Hartree−Fock theory. The DFT-B3LYP/6-31G method is adopted for the higher layer, as the species of interest involves a transition metal ion. In the course of optimizing the geometry of the active site with a few nearby residues, the lower layer has been treated by the UFF method.[34] The UFF method uses a charge equilibration scheme (QEq),[35] which enables charges to be generated dynamically in response to the environment and has been shown to reproduce atomic charges accurately for a variety of systems. Gaussian 98 on Windows (G98W)[36] was used in all these calculations. The effect of the interaction of protein dipoles and bare charges on the protein with the active site has been directly included into electronic energies by use of the two-layer ONIOM scheme (Figure 5). Unfortunately, the GAUSSIAN-98 software could not handle the whole of the protein. Therefore, the remainder of the protein was optimized by an Amber force field,[37] with DFT charges being used on the atoms. The Amber force field parameters generate accurate properties for large biomolecules such as proteins, nucleic acids, etc. Additionally, the Amber force field employs a dielectric constant for scaling down long-range coulomb interactions, which makes it ideal for optimizing the protein bulk that does not have any hetroatom. The electrostatic effects of the protein on the active site were now determined. The active site has once again been treated at a 6-31G level of theory. The protein is assumed to have an *effective* dielectric constant (ϵ_p), this being a good approximation as the protein interior is fairly hydrophobic.

Zhan et al.[38a] have determined the absolute hydration free energy of a proton in water. In our calculations, we make use of the value of hydration energy obtained by Zhan et al. to calculate the potential of the normal hydrogen electrode. The other species at the electrode, namely, molecular hydrogen, was optimized by using the DFT-B3LYP procedure, using the 6-31G(d) basis set. All molecular characteristics such as thermal energy and entropy were also calculated at this level of theory. Zhan et al. have also determined the hydration free energy of

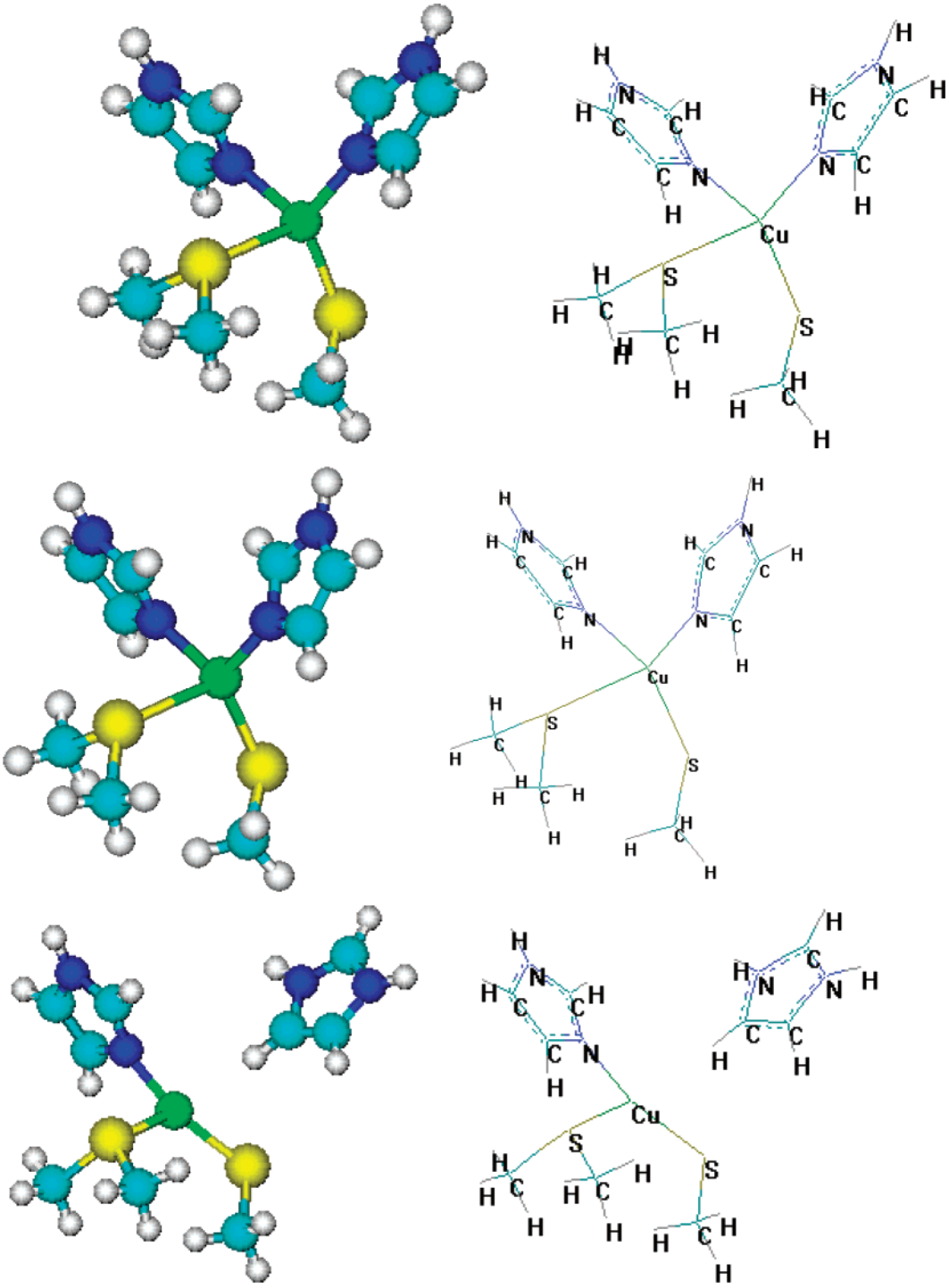

Figure 3. Systems chosen for thermal energy determination for the oxidized species (top) and the reduced species at pH values 7.0 (middle) and 3.8 (bottom).

the electron through a first principles approach.[38b] They have assigned a value of −35.5 kcal/mol to the free energy of electron hydration. This neglects the additional stabilization gained by an electron in a solution of an electrolyte due to formation of an ion cloud around the electron in accordance with Debye−Hückel theory. The hydration energy of the electron has been explicitly added, although the same energy has no direct bearing on the determination of reduction potential.

Systems representing the active sites and used to estimate the thermal energy and entropy for the species are shown in Figure 3. These calculations have also been carried out at the DFT/6-31G level. The thermal energy correction to the electronic energy incorporates the zero point energies for the system.

Medium Effects. The additional stability attained by a solvated species can be considered most efficiently by considering a dielectric continuum around it, and evaluating its interaction by using a self-consistent reaction field method.[39] However, the size of the protein is prohibitively large and does not permit such a calculation. Thus, the solvent medium, in this case water, has been treated as a dielectric continuum, and the energy of interaction of the protein with the solvent has been considered as the Born energy of ion−dielectric interaction and the Onsager energy of dipole−dielectric interaction.

Olsson and Ryde[40] performed extensive calculations on a model of the active site, $Cu(Im)_2(SCH_3)(S(CH_3)_2)$, where the histidines were replaced by imidazole moieties, the cysteine was

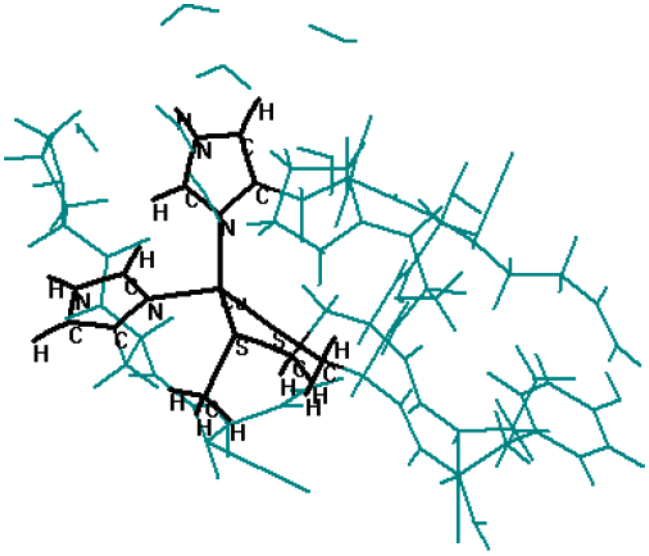

Figure 4. Complex chosen for the first set of ONIOM optimizations of the active site. The DFT layer is in dark, and the UFF layer is lightly shaded.

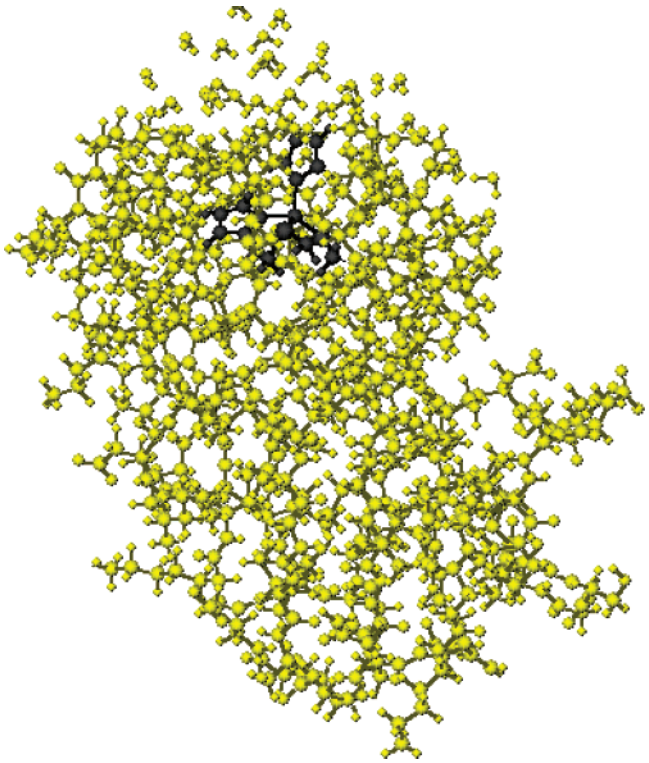

Figure 5. System chosen for the electronic energy calculations. The DFT layer is dark, and the Amber layer is lightly shaded.

represented as a methyl thiolate, and the methionine residue was modeled as dimethyl thioether. These authors suggested that the surrounding protein dipoles have an effect on the reduction potential. Solvation energy was calculated by the PCM method,[41] assuming a constant dielectric continuum of water around the complex. Olsson and Ryde calculated the relative reduction potentials for a number of Cu-containing proteins as differences of single point energies in the solvent (water), performed on the vacuum equilibrium geometries of the reduced and oxidized complexes. In their calculations, the reduction potential of plastocyanin was assumed at the experimental value, and relative to this value, the values of reduction potentials of other blue-copper proteins were determined.

In contrast, we are interested in computing the absolute value of the reduction potential of the whole protein in vitro and not the relative value for the active site dissolved in water. As discussed earlier, a direct SCRF treatment of the protein is not possible due to the prohibitively large size of the species. Also, because the active site is buried inside the protein and exposed to the solvent only on one side, and in turn the protein remains in solution, a direct SCRF or a PCM calculation would not give a true representation of the system. Any meaningful calculation would require an extensive change in the source code. Therefore, we have explicitly considered the Born energy as a first-order, perturbative effect.

Torres et al.[42a] have performed density functional studies on the redox potentials of Fe_4S_4 clusters. DFT optimized geometries were used to undertake redox potential calculations on the five known oxidation states of $[Fe_4S_4(SCH_3)_4]^{n-}$, where n lies between 0 and 4. The authors assumed the environment to be a continuum dielectric during the course of optimizations. The authors then used a standard set of radii and atomic charges to simulate the effect of protein dipoles on the active site. A triple-ζ basis set was used for 4s and 3d valence orbitals. A single 4p polarization function and 3s and 3p orbitals were used for iron, whereas 3s and 3p functions used on S atoms were augmented with a 3d polarization function.

Olsson et al.[42b] have recently investigated a frozen density functional free energy simulation of redox potentials of plastocyanin and rusticyanin. These authors have divided the protein into regions, which have been treated at differing levels of theory. Thus, the active site has been treated by the DFT methodology. The 63321/5211*/41+ basis set had been used for copper, the 73111/6111/1* basis set for sulfur, the 5211/411/1 basis set for oxygen, nitrogen, and carbon, and the 41/1 basis set for hydrogen. Other protein residues have been treated by the frozen DFT methodology, which assumes the electronic density to be frozen in space while the nuclei are free to move. For the fragments treated by FDFT, the smaller 6321/521 basis set was adopted for sulfur, and the 521/41 basis for oxygen, nitrogen, and carbon. The 41 basis set was used for hydrogen. The methodology and the basis sets used completely differ from those used in the present work. Two significant assumptions made by Olsson et al. are as follows: (i) The Cu−S bond length for the copper−cysteine thiolate linkage in the crystallographic geometry was retained in their calculations. (ii) The dielectric constant of the protein was taken to be 60 for the calculation of the charge−charge interaction energy between the ionized residues and the active site. The physical interpretation for such a high value of dielectric constant draws from the reorientation of charged residues of the protein.[42c,d] However, the protein plastocyanin has a hydrophobic interior, and hence a high degree of unfolding of the protein or reorientation of charged residues may be questionable. Indeed, plastocyanin is known to be a globular protein. Thus, the main emphasis of the work in ref 42b is to reproduce the differences in the reduction potentials of the two blue copper proteins plastocyanin and rusticyanin. Olsson et al. thus infer that the FDFT formalism is applicable to the determination of electronic properties of large systems.

The emphasis of the present work is to determine the value of the reduction potential of plastocyanin relative to the standard hydrogen electrode, as well as to determine its entropy of reduction at low pH values from its electrochemical properties. In our work, we have not imposed restrictions on the optimization of the copper−cysteine thiolate linkage. Molecular dynamics simulations have been undertaken to establish the appropriate dielectric constant for the protein in an aqueous solution. The

results of our molecular dynamical studies are discussed in detail in the appendix.

Ion−Dielectric Interaction. The Born energy of the protein in water is written as

$$E_{\mathrm{Born}}(\text{plastocyanin in water}) = -\frac{{z_p}^2 {e_o}^2}{2r_g}\left(1-\frac{1}{\epsilon_w}\right) \quad (2)$$

In the above, e_o is the electronic charge, ϵ_w is the dielectric constant of water, $z_p e_o$ is the net charge of plastocyanin (z_p is -8 for the oxidized form and for the reduced form at pH 3.8, and -9 for the reduced form at pH 7), and r_g is the effective radius for the protein plastocyanin, respectively.

The effective radius of plastocyanin was calculated from the crystallographic data. The dimensions of a unit cell are 29.6 Å × 46.86 Å × 57.6 Å (PDB code 1PLC). The volume of the molecule was found from the volume of the unit cell by considering the packing fraction $\pi/6$, that is,

$$\frac{4}{3}\pi {r_g}^3 = \frac{\pi}{6}abc \quad (3)$$

where a, b, and c are the side lengths of the unit cell. The value of r_g turns out to be 21.53 Å or 40.69 au (1 au = 0.529 177 Å). The solvent water molecules placed around the active site are additionally found to contribute 7765 au to the volume of the protein. Thus, the effective radius of the hydrated protein becomes 21.73 Å or 41.06 au. The normal practice, as in GAUSSIAN, is to add half the radius of the solvent molecule (water) to the molecular radius. Because there are highly polar regions in the exterior of the protein and these sites are considerably hydrated, we decided to add $^2/_3 r_w \pm {}^1/_6 r_w$, where $r_w = 0.96$ Å. Thus the effective radius r_g is found to be 22.37 ± 0.16 Å or 42.27 ± 0.30 au.

The inclusion of an adequate number (44) of water molecules about the active site of plastocyanin in the computational model effectively simulates the solvation of the imidazole moiety at pH 3.8. The dipole moments (μ) of the oxidized species, reduced species at pH 7, and reduced species at pH 3.8 are 73.00, 75.96, and 65.20 D, respectively. These values are obtained by summing over all the bond dipoles. The Onsager energy of interaction between the protein dipole and the solvent, given by

$$E_{\mathrm{Onsager}} = -\left[\frac{\epsilon_w - 1}{2\epsilon_w + 1}\right]\frac{\mu^2}{{r_g}^3} \quad (4)$$

can be estimated from the computed data. The Onsager term introduces a further correction of 12.0 mV to the reduction potential at pH 7, and a correction of −29.5 mV at pH 3.8. The estimate for the reduction potential at pH 7 after inclusion of the Onsager energy is thus 376 mV.

Dielectric Constant of the Interior of the Protein. Molecular dynamics studies on metal proteins such as myoglobin and cytochrome *f* have shown that proteins can be better considered as concentric shells of different effective dielectric constants, rather than one uniform dielectric constant.[43] Assuming that the protein is a sphere of two layers of concentric dielectric media, one for the highly polar surface (which makes the protein water soluble) and one for the hydrophobic interior, an expression was derived for the effective dielectric constant of the interior of the protein. The explicit derivation is given in Appendix I. The calculated value of ϵ_p, 8, was used in the calculation of the energy of electrostatic interaction between the distant residues and the protein active site.

Free Energy. For the smaller species involved in the reaction at the normal hydrogen electrode, the total internal energy is written as

$$E_{\mathrm{total}} = E_{\mathrm{SCRF}} + E_{\mathrm{DH}} + E_{\mathrm{Thermal}} \quad (5)$$

where E_{DH} is the Debye−Hückel energy of interaction of the ion with its ionic atmosphere,[44]

$$E_{\mathrm{DH}} = -\frac{{z_i}^2 {e_o}^2 \kappa}{2\epsilon_w} \quad (6)$$

The Debye−Hückel reciprocal length κ is given by

$$\kappa = \left[\frac{4\pi {e_o}^2}{\epsilon_w k_B T}\sum_i \left(\frac{Nc_i}{1000}\right){z_i}^2\right]^{1/2} \quad (7)$$

In the above, k_B is the Boltzmann constant, T is the temperature of the system in Kelvin, N is the Avogadro number, c_i is the concentration of the ith species in molar unit, and $z_i e_o$ is the charge of the ith ion. The energy E_{DH} is zero for water but finite for the aquated proton. No medium interaction energy is considered for the gaseous H_2.

The total energy of the protein is written as

$$E_{\mathrm{total}} = E_{\mathrm{ONIOM2}} + E_{\mathrm{Born}} + E_{\mathrm{Onsager}} + E_{\mathrm{Thermal}} \quad (8)$$

Here, E_{DH} was not considered because of the very low concentration of all ionic species.[9c]

The standard enthalpy $H°$ and the standard Gibbs free energy $G°$ are given by

$$H^o = E_{\mathrm{total}} + PV$$

and

$$G° = H° - TS° \quad (9)$$

Reductive Processes. We calculate the free energy for the overall process

$$\mathrm{H^+(aq) + e^-(aq) \rightarrow \frac{1}{2}H_2(g)} \quad (10)$$

Thus, for the smaller species involved in the reaction at the normal hydrogen electrode, the standard Gibbs free energy change is given by

$$\Delta G°\left[\mathrm{H^+(aq)/\frac{1}{2}H_2(g)}\right] = \Delta E_{\mathrm{SCRF/DFT}} + \Delta E_{\mathrm{DH}} + \Delta E_{\mathrm{thermal}} + k_B T\Delta n - T\Delta S° \quad (11)$$

per molecule, where Δn is the change in the number of species in the gas phase. This is equivalent to

$$\Delta G°\left[\mathrm{H^+(aq)/\frac{1}{2}H_2(g)}\right] = -\Delta G_{\mathrm{Hydration(proton)}} + \Delta E_{\mathrm{DH}} + \Delta G\left[\mathrm{H^+(g)/\frac{1}{2}H_2(g)}\right] \quad (12)$$

The reduction of PC^+(aq) can be considered to occur as follows. Above pH 5.5, the reaction is just the addition of an electron to the Cu atom,

$$\mathrm{PC^+(aq) + e^-(aq) \rightarrow PC(aq)} \quad (13)$$

whereas below pH 5.5, the reaction that takes place is the

TABLE 1: Calculation of the Gibbs Free Energy for the Hydrogen Smaller Species[a]

species	electronic energy (au)	thermal energy[b] (au)	Debye- Hückel correction (au)	total enthalpy[c] (au)	entropy (cal mol^{-1} K^{-1})	free energy (au)
H_2	−1.1755	0.0125		−1.1620	31.135	−1.1768
e^-(aq)		0.0014	−0.0011	0.0003		−0.0563[d]
H^+(aq)			−0.0011			−0.4192[e]

[a] We have used 1 au = 27.2116 eV and 1 eV = 23.0605 kcal mol^{-1}. [b] At 298.15 K (25 °C). [c] $H = E + kT$ for gaseous species; $H = E$ for solvated species. The thermal energy of an electron is $(3/2)kT$. [d] The free energy of hydration is −0.0566 au (from ref 38b). [e] This free energy is the sum of the free energy of hydration (−0.4181 au) from ref 38a and the Debye−Hückel energy of the charge−dielectric interaction.

TABLE 2: Molecular Characteristics for the Three Species PC^+, PC, and PCH^+ [a]

	ONIOM energy (au)[b]						
species	B3LYP/6-31G	electrostatic contribution[c]	total ONIOM	thermal energy (au)[d]	Born energy (au)[e]	Onsager energy (au)[e]	entropy[c] (cal mol^{-1} K^{-1})
PC^+ (Ox)	−3008.5186	2.2539	−3006.2647	0.2862	−0.7474 ± 0.0053	−0.0054	158.062
PC (red) (pH 7.0)	−3008.6688	2.3790	−3006.2899	0.2809	−0.9459 ± 0.0067	−0.0058	149.013
PCH^+ (red) (pH 3.8)	−3009.0785	2.2287	−3006.8498	0.2965	−0.7474 ± 0.0053	−0.0043	147.389

[a] We have used 1 au = 27.2116 eV and 1 eV = 23.0605 kcal mol^{-1}. [b] The values reported have been computed using an ONIOM2 technique with DFT-B3LYP method being used for the active site, and Amber force field for the remainder protein and solvent water molecules. [c] Calculated using the effective dielectric constant $\epsilon_p = 8.0$. [d] The values reported have been computed using the DFT-B3LYP method for the optimized active site. [e] The Born and Onsager energies have been calculated by taking the average radius 42.27 ± 0.30 au for PC and dielectric constant 78.5 for water at 25 °C.

TABLE 3: Calculation of $\Delta H°$ [a]

pH	reaction	ΔE_{ONIOM} (au)	$\Delta E_{Thermal}$ (au)	ΔE_{Medium} (au)	$\Delta H°$ (au)[a]
7.0	$PC^+(aq) + e^-(aq) \rightarrow PC(aq)$	−0.0252	−0.0067	−0.1990 ± 0.0014[b]	−0.2308 ± 0.0014
3.8	$PC^+(aq) + H^+(aq) + e^-(aq) \rightarrow PCH^+(aq)$	−0.5851	+0.0089	0.0011[b]	−0.1460[c]

[a] We have used 1 au = 27.2116 eV and 1 eV = 23.0605 kcal mol^{-1}. [b] $\Delta H° = \Delta E_{ONIOM} + \Delta E_{Thermal} + \Delta E_{Medium}$. [c] The ΔH term is negligibly small at pH 3.8 and pH 7. [d] After considering $\Delta H°$ for H^+(aq), −0.4290 au; $\Delta H° = \Delta G° + T\Delta S°$, where $\Delta G° = -0.4181$ au (from ref 38) and $\Delta S°$ is −23.01 cal mol^{-1} K^{-1} (from ref 46a).

addition of an electron to the Cu atom, accompanied by the dissociation of the imidazole side chain of the His87 residue and the protonation of the δ nitrogen on the same residue,

$$PC^+(aq) + H^+(aq) + e^-(aq) \rightarrow PCH^+(aq) \qquad (14)$$

For a specific process involving the larger species, $\Delta G°$ per reaction is written as

$$\Delta G° = \Delta E_{SCRF} + \Delta E_{Born} + \Delta E_{thermal} + k_B T\Delta n - T\Delta S \quad (15)$$

where Δn is again the change in the number of species in gas phase. The kinetic energy of the aquated electron was taken as that of the free (gaseous) electron. The standard potential for the reduction reaction is written as

$$E°_{red}\,(\text{in V}) = \left[-\Delta G° + \Delta G°\left(H^+(aq)/\frac{1}{2}H_2(g)\right)\right](\text{in eV}) \quad (16)$$

When protonation (or deprotonation) is involved, ΔG and the midpoint potential **E** will be pH-dependent. Because the reduction of plastocyanin at pH 3.8 involves the addition of a proton, the midpoint potential will be given by

$$E_{red}\,(\text{in V}) = E°_{red}\,(\text{in V}) - 2.303RT\text{pH}\,(\text{in eV}) \quad (17)$$

4. Results and Discussion

Aquated Proton. The free energy of hydration of the proton and that of the electron have been estimated by Zhan et al. to be −262.4 and −35.5 kcal/mol, respectively, from a first principles approach.[38a,b] The determination of the reduction potential of the proton has been evaluated using the above hydration energy. The electronic and thermal energies of gaseous hydrogen have been evaluated using the 6-31G(d) basis set. However, the hydration energy of the electron has no direct bearing on the determination of reduction potential, as both electrodes have water as the medium. The only residual medium interaction term arises form the Debye−Hückel contribution, because the ionic strengths of the solution at the two electrodes are different. This is evaluated to be −0.0011 au. The Debye−Hückel contribution toward the free energy of the proton at pH 3.8 is similarly evaluated to be −0.0011 au. The free energy calculated for process 10 is −0.1695 au (−4.612 eV). See Table 1.

Model Complex. The computed ONIOM energies and other characteristics of the model complexes are listed in Table 2. The thermal energies and entropies have been evaluated only for the DFT optimized active sites as discussed earlier.

The enthalpy changes associated with reactions 13 and 14 are listed in Table 3. As the species remain in the solvent medium, the PV contribution to enthalpy is exceedingly small and hence the $P\Delta V$ term has been neglected. The contribution of the electronic energy changes to the reduction potential has been considered to arise only from the changes in the active site.

Entropy Changes. The change in entropy stems from a variety of sources such as the change in the protein conformation and the reorganization of the solvent molecules around the protein. Hence, the entropy values computed for the isolated active site can account for only one part of ΔS. It is notoriously difficult to compute the entropy of a reaction, especially when one is considering a large molecule. The experimental value for the entropy change for the net reaction, that is, the reduction of plastocyanin and the simultaneous oxidation of H_2, was determined by Gray et al.[45] The observed value is −103.3 cal mol^{-1} K^{-1}. An estimate of the entropy of hydration of a proton has been obtained from the work of Noyes, who experimentally determined the value to be −25.36 cal $mol^{-1}K^{-1}$.[46a] From this, the ΔS value for the reduction of plastocyanin was calculated

TABLE 4: Calculation of the Reduction Potential of Plastocyanin[a]

					midpoint E (mV)	
pH	reaction	$\Delta H°$ (au)	$-T\Delta S$ (au)	calc ΔG (au)	calc	obs
0.0	$H^+(aq) + e^-(aq) \rightarrow {}^1/_2H_2(g)$			-0.1129[b]		
7.0	$PC^+(aq) + e^-(aq) \rightarrow PC(aq)$	-0.2308 ± 0.0014	$+0.0475$[c]	-0.1267 ± 0.0014[d]	376 ± 38	379[e]
3.8	$PC^+(aq) + H^+(aq) + e^-(aq) \rightarrow PCH^+(aq)$	-0.1460	-0.0478[f]	-0.1289[g]		436[h]

[a] We have used 1 au = 27.2116 eV and 1 eV = 23.0605 kcal mol^{-1}. [b] Using free energy of proton hydration and electron hydration from ref 43a,b. The Debye−Hückel correction has been introduced. [c] Observed value, ref 48. Only +0.0043 au can be accounted for by our calculation on the active site. Hence, 0.0432 au is due to the reorganization of the protein and surrounding water molecules during the reduction. [d] Using free energy of electron hydration −0.0566 au (ref 38b) without the Debye−Hückel term at pH 7. [e] Reference 9. [f] Estimated value that would give rise to the observed midpoint potential of 436 mV. Out of this value, 0.0051 au can be accounted for from the calculated entropies, −0.0109 au is due to the change of entropy of the proton on being attached, and −0.0420 au must arise from the reorganization of the protein and the water molecules surrounding it. [g] Using the free energy of hydration of electron −0.0566 au. (ref 38b) without the ΔH correction at pH 3.8, and $2.303RT$ pH = 0.0083 au. [h] Reference 6c. The value contains −2.303RT pH.

(−100.0 cal mol^{-1} K^{-1}), because the experimental value of entropy change for the oxidation of H_2 to an aqueous proton is known (−3.3 cal mol^{-1} K^{-1}).[46b] The calculated entropies of PC^+ and PC yields a ΔS value of only −9.05 cal mol^{-1} K^{-1}. Hence the remaining −90.95 cal mol^{-1} K^{-1} must account for the reorganization of water molecules around the active site and the small change in the protein conformation during the process of reduction. The entropy decreases as more molecules become associated on reduction.

Reduction Potential. The standard free energy changes for the reduction reaction is written as

$$\Delta G°_{red} = H°(PC) - H°(PC^+) - T\Delta S_{exp} \qquad (18)$$

at pH 7, where ΔS_{exp} is the experimental value for the reduction at pH 7. The reduction potential has been calculated for reaction 13. This calculation is shown in Table 4. The calculated potential (376 ± 38 mV) at pH 7 is in excellent agreement with the observed one (379 mV).[2]

Below pH 5.5, the free energy change is given by

$$\Delta G_{red} = H°(PCH^+) - H°(PC^+) - G°(H^+(aq)) - T\Delta S + 2.303RT\mathrm{p}H \qquad (19)$$

where the entropy change ΔS remains unknown. Because the midpoint potential is known (436 mV) at pH 3.8,[6] a similar calculation leads us to predict the entropy of reduction of plastocyanin at this pH to be +100.60 cal mol^{-1} K^{-1}. Out of this, −10.67 cal mol^{-1} K^{-1} can be accounted for from the calculated entropies of the involved species PCH^+ and PC (Table 2), and +23.01 cal mol^{-1} K^{-1} is attributable to the change of entropy of an aquated proton[46a] on being attached to the protein moiety. Therefore, 88.26 cal mol^{-1} K^{-1} accounts for the reorganization of water molecules around the active site and the change in protein conformation during the process of reduction.

5. Conclusions

A quantum chemical QM/MM calculation of the reduction potential of the protein plastocyanin from poplar leaves has been presented here. An ONIOM methodology has been adopted to divide the protein into smaller parts, based on their relative contributions to the reduction potential. Density functional methodology has been used for the active site, where there are major changes in electronic structure, whereas the remainder of the protein has been simulated by UFF and Amber force fields during the optimization of geometry and the single point energy evaluation, respectively. The fundamental structural features of the copper-containing protein have thus been retained during the course of geometry optimization of the species. The mechanism considered for the reaction above pH 5.5 is consistent with the reduction potential being independent of pH. The mechanism considered for the reduction below pH 5.5 agrees with the fact that the reduction potential increases by about 50−60 mV for each unit drop of pH.

The calculated potential (376 ± 38 mV) at pH 7 is in excellent agreement with the observed one (379 mV). The interaction with medium and the entropy change are found to play the crucial role in determining the potential. A similar calculation leads us to predict the entropy of reduction of PC at pH 3.8 to be +100.60 cal mol^{-1} K^{-1}. Thus, the reduction at low pH is associated with a large increase in entropy. This can be attributed to the following factors: (i) release of free water molecules on the attachment of a proton to the imidazole moiety of the complex; (ii) large change in the dipole moment of the considered species, which results in a change in water organization around the active site; (iii) change in the existing hydrogen bonding network around the rest of the protein. Our results are in conformity with the suggestion that the thermodynamic reasons for the acid transition (protonation in reduced form at low pH) are entropic for plastocyanins.[49]

Despite our apparent success in calculating the redox potential at pH 7, the present work must be understood as being subject to several limitations. The latter are as follows:

(i) The Debye−Hückel energy has been calculated for the aquated proton with unit activity. The linearization of the Poisson−Boltzmann equation is strictly valid at a much lower concentration that corresponds to a much shorter reciprocal length, which makes the use of the Debye−Hückel expressions (6) and (7) somewhat dubious. Still, the large dielectric constant of water gives rise to a Debye−Hückel contribution that is much smaller than the other solvation energy contributions. Nevertheless, the neglect of the Debye−Hückel term would cause the calculated reduction potential to decrease by approximately 60 mV.

(ii) The estimation of the entropy of reduction at pH 3.8 rests upon the assumption that the structure of the oxidized form of plastocyanin remains unchanged from the structure found at pH 6.

(iii) The geometry optimizations have been undertaken to an accuracy of 10^{-5} au in energy. The subsequent thermal energy calculation would at most introduce an inaccuracy of only a few millivolts into the computations.

Additionally, reduction potential calculations are found to be sensitive to the estimated radius of the protein. Thus, a change of ±0.1 au in the protein radius affects the change in Born energy by about ±0.0005 au. This causes the computed reduction potential to shift by ±13 mV. The calculation of the entropy of reduction of the protein at pH 3.8 is free from this error, because the net contribution of the Born term is zero in

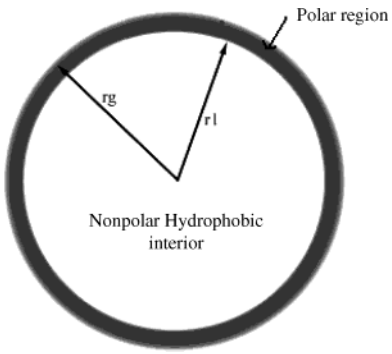

Figure 6. Schematic diagram for the protein in water, following ref 43a,b.

this case. Because of these reasons, the consideration of the Born energy as a first order correction suffices.

A more important factor is the dielectric constant in the interior of the solvated protein. The value of 8 adopted in this work has led to a more or less correct reduction potential at pH 7.0. This is rather fortuitous. Nevertheless, if ϵ_p changes by one unit from the value 8, the calculated potential changes by about 400 mV. Therefore, a very high value of ϵ_p in the bulk of plastocyanin is entirely unrealistic.

In short, the calculated electronic and solvent characteristics are in good agreement with the electronic structure of the Cu-containing region in the real specimen, plastocyanin. Determination of the rate of electron transfers from cytochrome*f* to plastocyanin and from plastocyanin to $P700^+$ is our ultimate objective and this work prepares the basis for our future work in this direction.

Acknowledgment. We thank the reviewers for making a large number of critical and valuable suggestions.

Appendix I: Evaluation of the Dielectric Constant of the Interior of a Protein

The explicit derivation of an effective dielectric constant (ϵ_1) for the inner side of a globular protein is described here. Molecular dynamics has provided several insights into the effect of charge screening in proteins.[43a,b] Results from molecular dynamics indicate that the dielectric constant of a protein can be hardly understood from the dielectric constant values obtained from the physical measurements undertaken on dry powders of proteins. Two important factors that affect the dielectric constant of a protein in solution are (i) the ionization of residues containing carboxylate and amino groups and (ii) the interaction of solvent with the outer layers of the protein. Following the molecular dynamical investigations in ref 43a,b, a globular protein can be modeled as a sphere with two concentric shells having different dielectric constants. For a water soluble protein such as plastocyanin, the outer layer is highly polar, with dielectric constant ϵ_2. We take ϵ_p as the net dielectric constant of the protein, which is to be determined. Besides, r_g is the effective radius of the whole entity, and r_1 is the effective radius of the inner shell, as shown in Figure 6.

As shown in Figure 2, the active site is located in the outer layer. The charged residues are also located in the outer periphery of the protein. Consequently, the effective dielectric constant of the protein must be determined and considered for the evaluation of the energy of interaction of the charge and the dipoles in the bulk with the active site. The effect and the degree of solvation of the outer peripheral layer of the protein were estimated from a molecular dynamics study of the oxidized form of the protein. Whereas the precise determination of the dielectric constant of a protein is still not possible, this method allows for an estimation of the effective dielectric constant of the protein in solution. Simonson et al. have discussed that there is an error of about 3 in the estimation of dielectric constant by a molecular dynamics technique.

We undertook a 100 ps simulation on a section of the protein to estimate the approximate degree of penetration of water into the protein. Altogether 640 water molecules were taken into consideration. The MM+ force field was chosen for the molecular dynamics simulation, as it is an all atom force field, which enables placing of quantum mechanically computed charges on the atoms. This force field includes cutoffs for nonbonded interactions, which makes it a very general force field for solvation and molecular dynamics simulations.[47] The protein was first optimized using an MM+ force field and the DFT generated charges on the solvent (water) molecules and the protein. The MM+ force field was then used to simulate the dynamics of a section of the protein in water at 300 K, in steps of 0.002 ps. Hyperchem Professional Release 7 for Windows[47] was used in these calculations. The results show that the water molecules effectively penetrate into a layer of thickness in range of 4−10 au into the protein. This is shown by the shaded region in Figure 6.

Simonson et al. have discussed that the outer layer generally has an effective dielectric constant of 20. The dielectric constant of dry cytochrome *c* powder is 3.6.[44b] Hence the average dielectric constant can be estimated as

$$\epsilon_p = \frac{r_1^3\epsilon_1 + (r_g^3 - r_1^3)\epsilon_2}{r_g^3} \qquad \text{(A.1)}$$

As discussed in the text, the effective radius of the protein (r_g) is 42.27 au. Therefore, the average dielectric constant in the bulk is found in the region of 7.8−12.7 for $r_g - r_1 = 4-10$ au. The value of 12.7 is certainly an overestimation, as only a few water molecules penetrate up to a thickness of 10 au. The lower average value 8 has been used in the text, as most of the solvent penetration extends up to approximately 4 au.

References and Notes

(1) Redinbo, M. R.; Cascio, D.; Chonkair, M. K.; Rice, D.; Merchant, S.; Yeates, T. O. *Biochemistry* **1993**, *32*, 10560.

(2) Katoh, S.; Shiratori, I.; Tahamiya, A. *J. Biochem. (Tokyo)* **1962**, *51*, 32.

(3) Fee, A. J. *Structure Bonding*; Springer: Berlin, 1975; Vol. 23, p 60. Colman, P. M.; Freeman, H. C.; Guss, J. M.; Murata, M.; Norris, V. A.; Ramshaw, J. A. M.; Venkatappa, M. P. *Nature* **1978**, *272*, 319.

(4) Sykes, A. G. *Adv. Inorg. Chem.* **1991**, *36*, 377. Machonkin, T. E.; Zhang, H. H.; Hedman, B.; Hodgson, K. O.; Solomon, E. I. *Biochemitsry* **1998**, *37*, 9570.

(5) Guss, J. M.; Harrowell, P. R.; Murata, M.; Norris, V. A.; Freeman, H. C. *J. Mol. Biol.* **1986**, *192*, 361.

(6) (a) Beinert, H. *Coord. Chem. Rev.* **1980**, *33*, 55. (b) Guss, J. M.; Freeman, H. C. *J. Mol. Biol.* **1983**, *169*, 521. (c) Buchi, F. N.; Bond, A. M.; Codd, R.; Huq, L. N.; Freeman, H. C. *Inorg. Chem.* **1992**, *31*, 5007.

(7) Segal M. G.; Sykes, A. G. *J. Am. Chem. Soc.* **1978**, *100*, 4584.

(8) (a) Markley, J. L.; Ulrich, E. L.; Krogmann, D. W. *Biochem. Biophys. Res. Commun.* **1977**, *78*, 106. (b) Freeman, H. C.; Norris, V. A.; Ramshaw, J. A. M.; Wright, P. E. *FEBS Lett.* **1978**, *86*, 131.

(9) Datta, S. N.; Priyadarshy, S. *Chem. Phys. Lett.* **1990**, *173*, 360.

(10) Mallik, B.; Datta, S. N. *Int. J. Quantum Chem.* **1994**, *52*, 629.

(11) Datta, S. N.; Mallik, B. *Int. J. Quantum Chem.* **1995**, *53*, 37; **1997**, *61*, 865.

(12) Datta, S. N.; Mallik, B. *J. Phys. Chem. B* **1997**, *101*, 4171, 5191. Datta, S. N.; Prabhakar, B. G. S.; Nehra, V. *J. Phys. Chem. B* **1999**, *103*, 2291. Datta, S. N.; Nehra, V.; Jha, A. *J. Phys. Chem. B* **1999**, *103*, 8768. Datta, S. N.; Parandekar, P. V.; Lochan, R. C. *J. Phys. Chem. B* **2001**, *105*, 1442.

(13) Datta, S. N.; Deshpande, R. *Ind. J. Pure Appl. Phys.* **1997**, *35*, 483.
(14) (a) Garrett, T. P. J.; Clingeleffer, D. J.; Guss, J. M.; Rogers, S. J.; Freeman, H. C. *J. Biol. Chem.* **1984**, *259*, 2822. (b) Guckert, J. A.; Lowery, M. D.; Solomon, E. I. *J. Am. Chem. Soc.* **1995**, *117*, 2817. (c) De Kerpel, Jan, O. A.; Ryde, U. *Proteins: Struct., Funct., Genet.* **1999**, *36* (2), 157.
(15) Kurnikov, I. V. Beratan, D. N. *J. Chem. Phys.* **1996**, *105*, 9561.
(16) Newton, M. D. *Int. J. Quantum. Chem. Symp.* **1980**, *14*, 363.
(17) Logan, J.; Newton, M. D. *J. Chem. Phys.* **1983**, *78*, 4086.
(18) Balaji, V.; Jordan, K. D.; Burrow, P. D.; Paddon-Row, M. N.; Patney, H. K. *J. Am. Chem. Soc.* **1982**, *104*, 6849.
(19) Jordan, K. D.; Paddon-Row, M. N. *Chem. Rev.* **1992**, *92*, 395.
(20) Mikkelsen, K. V.; Ratner, M. A. *J. Phys. Chem.* **1989**, *93*, 1759.
(21) Gruschus, J. M.; Kuki, A. *J. Phys. Chem.* **1993**, *97*, 5581.
(22) Larsson, S.; Volosov, A. *J. Chem. Phys.* **1987**, *87*, 6623.
(23) Beratan, D. N.; Hopfield, J. J. *J. Am. Chem. Soc.* **1984**, *106*, 1584.
(24) Beratan, D. N.; Onuchic, J. N.; Hopfield, J. J. *J. Chem. Phys.* **1987**, *86*, 4488.
(25) Priyadarshy, S.; Skourtis, S. S.; Risser, S. M.; Beratan, D. N. *J. Chem. Phys.* **1996**, *104*, 9473.
(26) Larsson, S. *J. Am. Chem. Soc.* **1981**, *103*, 4034; *J. Chem. Soc., Faraday Trans. 2* **1983**, *79*, 1375; *Chem. Phys. Lett* **1982**, *90*, 136; *J. Phys. Chem.* **1984**, *88*, 1321.
(27) Ratner, M. A. *J. Phys. Chem.* **1990**, *94*, 4877.
(28) Broo, A.; Larsson, S. *J. Phys. Chem.* **1991**, *95*, 4925.
(29) Stuchenbrukhov, A. A.; Marcus, R. A. *J. Phys. Chem.* **1995**, *99*, 7581.
(30) Evenson, J. W.; Karplus, M. *J. Chem. Phys.* **1992**, *96*, 5272.
(31) Ryan, J. J.; Risser, S. M.; Beratan, D. N.; Onuchic, J. N. *J. Phys. Chem.* **1993**, *97*, 13083.
(32) Siddarth, P.; Marcus, R. A. *J. Phys. Chem.* **1992**, *96*, 3213; *J. Phys. Chem.* **1993**, *97*, 2400; *J. Phys. Chem.* **1993**, *97*, 6111.
(33) Svensson, M.; Humbel, S.; Froese, R. D. J.; Matsubara, T. *J. Phys. Chem.* **1996**, *100*, 19357.
(34) Rappe, A. K.; Casewit, C. J.; Colwell K. S.; Goddard, W. A., III; Skiff, W. M. *J. Am. Chem. Soc.* **1992**, *114*, 10024.
(35) Rappe, A. K.; Goddard, W. A., III. *J. Phys. Chem.* **1991**, *95*, 3358.
(36) Frisch, M. J.; Trucks, G. W.; Schlegel, H. B.; Scuseria, G. E.; Robb, M. A.; Cheeseman, J. R.; Zakrzewski, V. G.; Montgomery, J. A., Jr.; Stratmann, R. E.; Burant, J. C.; Dapprich, S.; Millam, J. M.; Daniels, A. D.; Kudin, K. N.; Strain, M. C.; Farkas, O.; Tomasi, J.; Barone, V.; Cossi, M.; Cammi, R.; Mennucci, B.; Pomelli, C.; Adamo, C.; Clifford, S.; Ochterski, J.; Petersson, G. A.; Ayala, P. Y.; Cui, Q.; Morokuma, K.; Malick, D. K.; Rabuck, A. D.; Raghavachari, K.; Foresman, J. B.; Cioslowski, J.; Ortiz, J. V.; Stefanov, B. B.; Liu, G.; Liashenko, A.; Piskorz, P.; Komaromi, I.; Gomperts, R.; Martin, R. L.; Fox, D. J.; Keith, T.; Al-Laham, M. A.; Peng, C. Y.; Nanayakkara, A.; Gonzalez, C.; Challacombe, M.; Gill, P. M. W.; Johnson, B. G.; Chen, W.; Wong, M. W.; Andres, J. L.; Head-Gordon, M.; Replogle, E. S.; Pople, J. A. *Gaussian 98*, revision A.11.4; Gaussian, Inc.: Pittsburgh, PA, 1998.
(37) Cornell, W. D.; Cieplak, P.; Bayly, C. I.; Gould, I. R.; Merz, K. M., Jr.; Ferguson, D. M.; Spellmeyer, D. C.; Fox, T.; Caldwell, J. W.; Kollman, P. A. *J. Am. Chem. Soc.* **1995**, *117*, 8897.
(38) (a) Zhan, C. G.; Dixon, D. A. *J. Phys. Chem. A* **2001**, *105*, 11534. (b) Zhan, C. G.; Dixon, D. A. *J. Phys. Chem. B* **2003**, *107*, 4403.
(39) Newton, M. D. *J. Phys. Chem.* **1975**, *79*, 2795.
(40) Olsson, M. H. M.; Ryde, U. *J. Biol. Inorg. Chem.* **1999**, *4*, 654.
(41) Tomasi, J.; Persico, M. *Chem. Rev.* **1994**, *94*, 2027.
(42) (a) Torres, R. A.; Lovell, T.; Noodleman, L.; Case, D. A. *J. Am. Chem. Soc.* **2003**, *125* (7), 1923. (b) Olsson, M. H. M.; Hong, G.; Warshel, A. *J. Am. Chem. Soc.* **2003**, *125*, 5025. (c) Johnson, E. T.; Parson, W. W. *Biochemistry* **2002**, *41* (20), 6483. (d) Claudia, S. N.; Warshel, A. *Proteins: Struct., Funct., Genet.* **2001**, *44* (4), 400.
(43) (a) Simonson, T.; Brooks, C. L., III. *J. Am. Chem. Soc.* **1996**, *118*, 8452. (b) Simonson, T.; Perahia, D. *Proc. Natl. Acad. Sci. U.S.A.* **1995**, *92*, 1082.
(44) Bockris, J. O'M; Reddy, A. K. N. In *Modern Electrochemisrty*; Plenum Press: New York and London, 1998; p 565.
(45) Napanon, S.; Anson, F. C.; Gray, H. B. *J. Am. Chem. Soc.* **1979**, *101*, 455.
(46) (a) Noyes, R. M. *J. Am. Chem. Soc.* **1962**, *84* (4), 513. (b) Battistuzzi, G.; Borsari, M.; Canters, G. W.; Waal, E. de; Leonardi, A.; Ranieri, A.; Sola, M. *Biochemistry* **2002**, *41*, 14293.
(47) HyperChem Professional Release 7.01 for Windows; Hypercube Inc., Gainesville, FL, 2002.